Biosensors and Bioelectronics 103 (2018) 158–162

Contents lists available at ScienceDirect

Biosensors and Bioelectronics

journal homepage: www.elsevier.com/locate/bios

Photonic crystals on copolymer film for label-free detection of DNA hybridization

Han Su[a], Xin R. Cheng[a], Tatsuro Endo[b], Kagan Kerman[a,*]

[a] Dept. of Physical and Environmental Sciences, University of Toronto Scarborough, Toronto, ON, Canada M1C 1A4
[b] Dept. of Applied Chemistry, Osaka Prefecture University, 1-1 Gakuen-cho, Naka-ku, Sakai-shi, Osaka 599-8531, Japan

ARTICLE INFO

Keywords:
Photonic crystal
DNA
LSPR
Reflectance
Absorbance
Apolipoprotein E
Biosensor

ABSTRACT

The presence of a single-nucleotide polymorphism in Apolipoprotein E4 gene is implicated with the increased risk of developing Alzheimer's disease (AD). In this study, detection of AD-related DNA oligonucleotide sequence associated with Apolipoprotein E4 gene sequence was achieved using localized-surface plasmon resonance (LSPR) on 2D-Photonic crystal (2D-PC) and Au-coated 2D-PC surfaces. 2D-PC surfaces were fabricated on a flexible copolymer film using nano-imprint lithography (NIL). The film surface was then coated with a dual-functionalized polymer to react with surface immobilized DNA probe. DNA hybridization was detected by monitoring the optical responses of either a Fresnel decrease in reflectance on 2D-PC surfaces or an increase in LSPR on Au-coated 2D-PC surfaces. The change in response due to DNA hybridization on the modified surfaces was also investigated using mismatched and non-complementary oligonucleotides sequences. The proof-of-concept results are promising towards the development of 2D-PC on copolymer film surfaces as miniaturized and wearable biosensors for various diagnostic and defense applications.

1. Introduction

DNA sensing studies traditionally involve solid-phase hybridization assays (Kang et al., 2010; Tel-Vered et al., 2012; Wang, 2005). These techniques typically employ an enzyme or nanoparticle-tagged secondary oligonucleotide binding to surface-immobilized DNA for either optical or electrochemical detection, thereby converting the hybridization event to a quantifiable signal. However, the detection of DNA hybridization by secondary probes is intrinsically complex, time-consuming and requires multiple layers of interacting components with high specificity. As a result, the detection of primary DNA hybridization would greatly simplify routine DNA assays. Label-free measurement of bioaffinity events is a potentially powerful tool, simpler and more efficient than secondary probe-based systems. In the past decade, our group and others have demonstrated the label-free detection of various clinically important biomolecules using electrochemical and optical biosensors (Aygun et al., 2017; Cheng et al., 2014; Ember et al., 2011; Endo et al., 2005a, 2005b; Huang et al., 2018; Kaatz et al., 2012; Kim et al., 2008; Ozkumur et al., 2010; Spuhler et al., 2010; Yurt et al., 2012).

In this report, a novel sensing surface comprising of photonic crystals (PCs) is introduced as a promising platform for optical detection of DNA hybridization. PCs are periodic optical nanostructures that possess a periodic dielectric structure with a photonic band gap, which does not allow light propagation of a specific wavelength range (John, 1987; Yablonovitch, 1993). Such control and manipulation of light allows optical communication applications to be studied experimentally according to Bragg's Law (Vlasov et al., 2005). The optical properties of PCs are related to their periodicity, size and average refractive index (Xu and Asher, 2004). Conveniently, these characteristics can be easily controlled using nano-imprint lithography (NIL). This printable photonics technology allows the fabrication of structural features down to the nanometer level using highly homogenous polymers (Endo et al., 2010, Aki et al., 2014; Guo, 2007).

In this study, DNA hybridization was detected by monitoring the Fresnel reflection change (Endo et al., 2010). Fresnel reflection is observed by the behavior of light travelling through media of varying refractive indices. Since the reflection peak wavelength is detected within the visible region, 2D-PC creates a promising and simple sensing platform. This emerging technology has been successfully applied towards the development of selective and sensitive biosensors (Alexeev et al., 2003; Aki et al., 2014; Cheng et al., 2014; Endo et al., 2008a, 2008b, 2010; Inan et al., 2017; Ma et al., 2009; Liu et al., 2017; Sharma et al., 2004). The multiplexed detection of cancer biomarkers was reported using quartz-based photonic crystal surfaces (Huang et al., 2012). We have also achieved the observation of a localized surface

* Corresponding author.
E-mail address: kagan.kerman@utoronto.ca (K. Kerman).

https://doi.org/10.1016/j.bios.2017.12.013
Received 16 August 2017; Received in revised form 9 November 2017; Accepted 7 December 2017
Available online 14 December 2017
0956-5663/

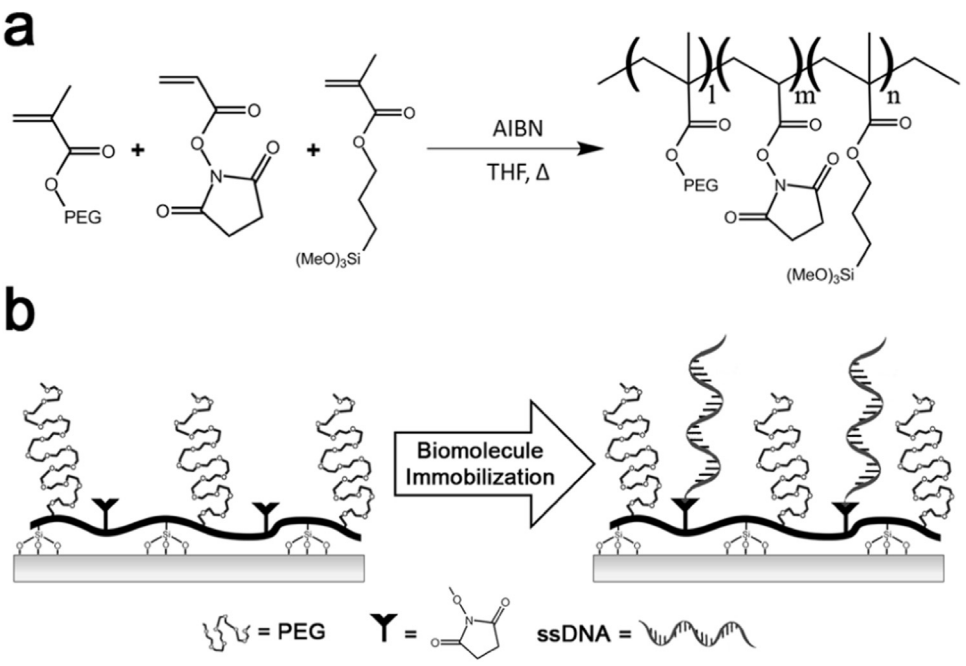

Fig. 1. (a) Synthetic scheme for the production of the multi-functional film, which contained l) protein-resistive, m) bio-reactive and n) anchor groups. (b) Schematic representation for specific immobilization of probe ssDNA on the multi-functional film.

plasmon resonance (LSPR) band by coating the surface of 2D-PC with a thin layer of Au. Noble metal nanoparticles exhibit rich LSPR properties from the collective oscillation of conduction electrons in response to optical excitation (Anker et al., 2008; Sagle et al., 2011). Stability and dispersion of deposition is difficult to control for nanoparticles significantly larger than 10 nm (McMahon and Emory, 2006; Park and Park, 2008). This problem was easily resolved, when Au sputtering was performed on the 2D-PC to form homogenously spaced Au nanostructures that produced an intense LSPR response for the first time in this report. As proof of principle, Apolipoprotein E gene (ApoE) was detected on these novel 2D-PC surfaces. Human ApoE is present in three isoforms (E2, E3 and E4) and related to two polymorphic codon sites (112 and 158) of the gene located on chromosome 19 (Bellis et al., 1997). These isoforms arise from 3 alleles: ε2, ε3 and ε4 (Siest et al., 1995). ApoE isoforms have been found in patients with type-III hyperlipidemia, atherosclerosis and Alzheimer's disease (AD) (Corder et al., 1993; Deming et al., 2015; Farrer et al., 1997; Morris et al., 2010). Inheritance of the ApoE single nucleotide polymorphisms is the only confirmed and consistently replicated risk factor for late-onset AD (Venter et al., 2001). Cramer et al. (2012) have recently reported that ApoE-directed therapeutics rapidly cleared amyloid-β deposits and reversed deficits in AD mouse models. Thus, reliable sensing platforms for ApoE gene is in high demand for the development of future AD therapeutics (Cramer et al., 2012; Landreth et al., 2013; Venter et al., 2001). Reports about the biosensor development for ApoE gene included electrochemical detection on disposable screen-printed electrodes (Ahmed et al., 2007; Marrazza et al., 2001), piezoelectrical detection on quartz crystals (Marrazza et al., 2000; Tombellis et al., 2000) and peptide nucleic acids in connection with electrochemical impedance spectroscopy (Guo et al., 2011). Compared to the previous methods of detection, the development of this novel ApoE sensor could potentially facilitate the development of cost-effective disposable biosensors in detection of clinically important biomolecules (Endo et al., 2016). Here, we report the fabrication and proof-of-concept results of a DNA hybridization sensor based on 2D-PC and Au-coated 2D-PC surfaces.

2. Materials and methods

2.1. Reagents

The oligonucleotides were purchased from BioBasic, Inc. (Markham, ON) as sodium salts. The probe was a 5′ disulfide-modified 23-bp long sequence from a fragment of the allele ε2 around codon 158. Fully complementary target DNA (FC), mismatch DNA (MM- single nucleotide polymorphism underlined) and non-complementary DNA (NC) were used in this study:

5′ to 3′:HS-S- ACC TGC AGA AGC GCC TGG CAG TG Probe
CAC TGC CAG GCG CTT CTG CAG GT FC
CAC TGC CAG GCA CTT CTG CAG GT MM
GAT TAG AGT CCC GCA ATT AAT CAT T NC

For the thiolated probes, the immobilization buffer was 1 M KH_2PO_4, (pH 3.8). Hybridization buffer contained 300 mM NaCl, 20 mM Na_2HPO_4, 0.1 mM EDTA (pH 7.4). All other reagents, unless stated otherwise were used as received from Sigma-Aldrich (Oakville, ON). EDTA and Tris-HCl were obtained from BioBasic Inc. (Markham, ON). In addition, ultra-pure water (18.3 MΩ cm) from Pall Cascada water purification systems was used in all preparations.

2.2. Fabrication and design of 2D-PC using nano-imprint lithography (NIL)

The mold for heat transfer was fabricated using computer aided design (CAD) system, electron-beam lithography, and nickel electrocasting. The film was prepared on ZeonorFilm ZF14 for NIL. After the fabrication of mold, heat transfer was performed using a semi-automatic nano-imprint apparatus (SCIVAX Corp. Ltd., Kanagawa, Japan, X-300). The co-polymer surface was pre-modified with dual functionality (Fig. 1a), which comprised of a protein resistant part (polyethylene glycol), anchor part (trimethoxysilane) and a bio-reactive part (N-acryloxysuccinimide). 2,2′-azobisisobutyronitrile (AIBN) and tetrahydrofuran (THF) were used as solvents (Ozkumur et al., 2010; Park et al., 2007). Then, 2D-PC film was immersed in a polymer solution that functionalized the surface with bio-inert (Siest et al., 1995) and bio-reactive properties. This provided anti-fouling characteristics on the film surface as well as sites that can bind to biomolecules. (Fig. 1b). For

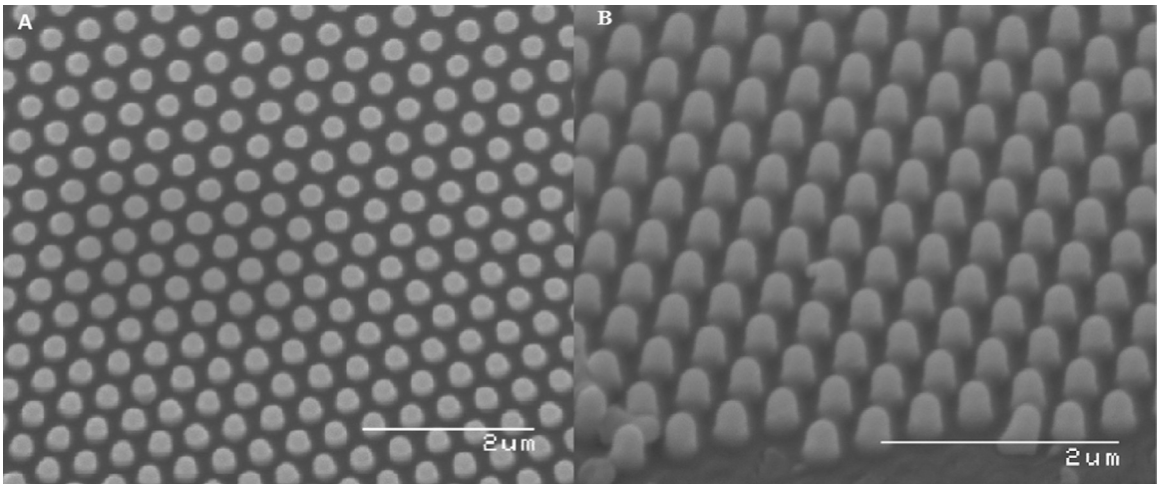

Fig. 2. (A) SEM images of the top-down view and (B) 35° angled-view of Au fingers-like nanostructures on the 2D-PC surface.

the Au-coated 2D-PC, Au sputtering was performed with SEM coating unit PS3 (Agar Scientific) at 19 mA plasma current for 100 s.

2.3. Optical measurements

The optics system set up is composed of a spectrophotometer (USB-4000-UV–Vis), a tungsten halogen light source (LS-1-LL, wavelength range 200–1100 nm), a fiber probe bundle (fiber core diameter 400 μm, wavelength range 300–1100 nm) and WS-1 diffuse reflectance standard, all purchased from Ocean Optics. (Dunedin, USA) The diffuse reflectance standard was used as a Lambertian reference surface. The UV–Vis probe was placed close to the working electrode surface so that incident light was reflected upon hitting the surface and then backed in the detector situated in the light probe. The Reflectance and Absorbance Mode of the Spectra Suite software was used to measure the spectral characteristics of the samples for the 2D-PC reflectance and Au-coated 2D-PC absorbance, respectively. The intensity and wavelengths of spectral peaks were recorded as modifications were made to the surface. The probe height was held constant (~ 1 mm above sample surface) throughout study. All experiments were performed at room temperature. (23 ± 2 °C).

2.4. Microscopy

Atomic force microscopy (AFM) for surface analysis of the 2D-PC was performed using a commercial AFM unit 35 (SPA-400, Seiko Instruments, Inc., Chiba, Japan) with a calibrated 20 μm xy-scan and 10 μm z-scan range PZT-scanner. AFM was carried out in tapping mode using silicon tips and cantilevers with a nominal spring constant of 13 N/m for scanning in air. All reported images were acquired at scan rates in the range 0.25–0.50 Hz. Au sputtering was performed with SEM coating unit PS3 (Agar Scientific) at 19 mA plasma current for 100 s. The 2D-PC was then electrically connected to the sample stub by smearing silver paste dissolved in acetone from the sample to the metallic stub. The surface was also observed with a Hitachi S530 scanning electron microscope (SEM) at acceleration voltage of 20 kV and a working distance of 5.0 mm.

2.5. DNA immobilization and hybridization

The immobilization of probe ssDNA was done by incubating (20 μM) in 1 M KH_2PO_4, (pH 3.8) in a moist environment for 24 h, and then immersing in 100 mM borate buffer (pH 8.5) for 1 h to hydrolyze and deactivate unreacted N-acryloxysuccinimide sites. The covalent attachment of DNA on the surface was through primary amine groups on cytosine, guanine and adenine. After probe immobilization, 5 μM target ssDNA were introduced in 20 mM Na_2HPO_4 with 0.1 mM EDTA and 300 mM NaCl (pH 7.4) for 12 h. Tween-20 (0.1% w/v) in 20 mM Tris-HCl was used as washing buffer to remove non-specifically bound DNA. The surface was then rinsed with copious amount of water. For the Au-coated 2D-PC, the same procedure as above was performed, and the strong affinity between Au and the thiolated oligonucleotides was used for the immobilization of probe ssDNA. At least triplicate measurements were performed for all the DNA samples (n = 3).

3. Results and discussion

Initially, the surface characteristics of 2D-PC were studied using AFM and SEM. In the AFM images of the 2D-PC surface, it was observed that highly periodic and homogenous structures were inscribed successfully onto the copolymer surface using NIL. The holes on the 2D-PC surface with 230 nm i.d. collectively produced a visible color of violet-blue. The 2D-PC was placed under the fiber optic probe, and two peak reflection wavelengths were observed at 420 and 440 nm. After Au sputtering to facilitate SEM imaging, the surface was visually observed to change from a semi-transparent film to a shiny red surface. The reflectance peak wavelength was red-shifted to 650 nm, which supported the color of surface observed. From the SEM image, finger-like protrusions of 2D-PCs were observed (Fig. 2). These structures acted like nanostructures that collectively produced an LSPR signal when excited by light (Endo et al., 2005a, 2005b; Vlasov et al., 2005). However, the uniformity of 2D-PC nanostructures that were created using NIL produced more reproducibility between surfaces from batch-to-batch with a sharper LSPR band.

By having the dual-functional copolymer surface on the surface, non-specific adsorption could be greatly reduced (Jon et al., 2003). The bio-reactive groups of the surface formed strong ester linkages with the ssDNA probe that contained primary amine groups. After immobilization of the ssDNA probe, the 2D-PC was monitored under the optical probe. A prominent decrease in reflection intensity of 24.2 ± 5.1% in comparison with the blank surface was observed (Fig. 3A). This showed that the surface responded to the immobilization of ssDNA probe, and the decrease in reflection intensity was due to the increase in refractive index of surface film due to the ssDNA layer. Subsequent additions of DNA probes and their corresponding changes in reflectance intensity compared to control surface were summarized in Fig. 3B. Washing the incubated surfaces in diluted detergent solutions reduced non-specific binding. It was shown that the 420 nm peak decreased by 67.1 ± 2.8% after FC target oligonucleotide hybridized with the probe on the surface. This significant decrease corresponded to the DNA hybridization on the surface, which altered the surface refractive index. However, the binding of the NC and MM resulted in the decrease in reflectance

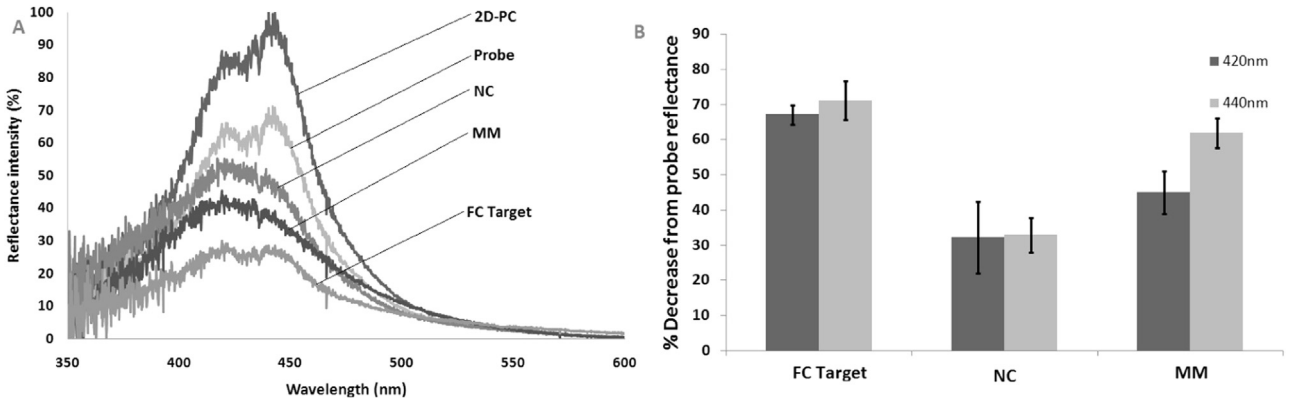

Fig. 3. (A) Reflectance intensity against wavelength to show decrease in Fresnel signal as different target oligonucleotides were exposed to the surface-immobilized ApoE probe on 2D-PC surface. (B) Variations in reflectance intensity with respect to the ApoE probe immobilized surface against different oligonucleotides. The changes in reflectance intensity were monitored at the two peak wavelengths of 420 nm and 440 nm.

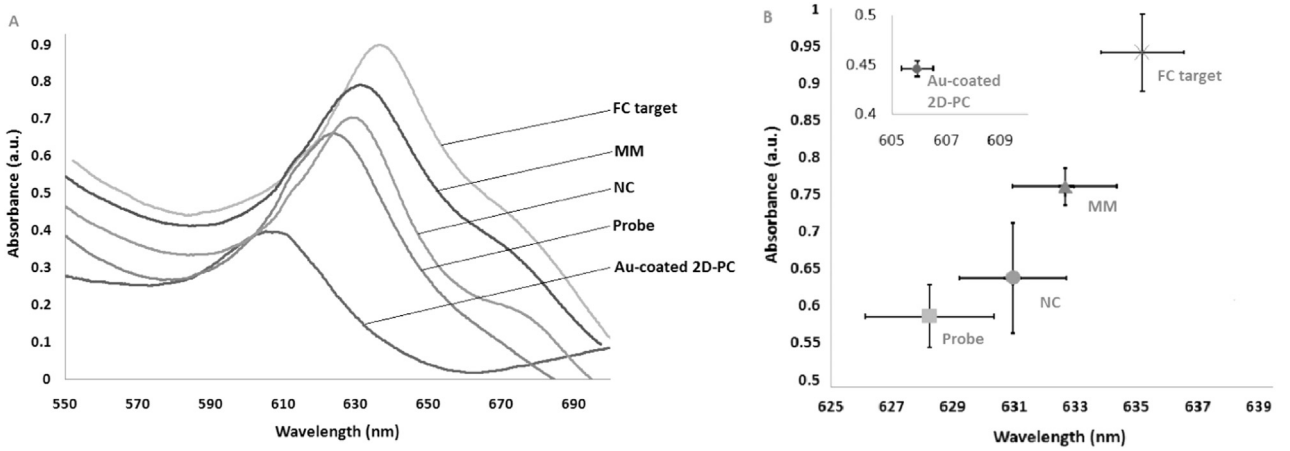

Fig. 4. (A) LSPR spectra observed on Au-coated 2D-PC surface after the immobilization of ApoE probe and various target oligonucleotides. (B) Variations in LSPR peak wavelengths and intensities as different target oligonucleotides were hybridized with the surface-immobilized ApoE probe.

intensity by 32.1 ± 10.2% and 45.0 ± 6.04%. This showed that the surface could be used to distinguish FC and NC. However, MM had a standard deviation that overlapped with that of NC. This was probably because of the similar nature that they could not bind specifically to the probe to form stable duplexes. The higher average decrease in reflectance intensity by MM compared to NC could still be a good indication of the binding efficiency to the probe-immobilized surface. A similar trend was observed for the shoulder peak that was recorded at 440 nm.

The promising results obtained on the reflective properties of 2D-PC surface led to idea of studying LSPR-based assays on the same surface. Au sputtering was performed on the 2D-PC (de Harven et al., 1984). The observed red shiny surface resembled the surface produced from Au-capped nanoparticles (Endo et al., 2005a, 2005b). It is known that the uniformity of Au nanostructures on surfaces affected the width and sensitivity of the LSPR band (Hutter and Fendler, 2004; Jung and Frey, 2015; Lee and Choi, 2010; Sepúlveda et al., 2009). In this case, Au-coated finger-like protrusions were expected to produce a similar LSPR effect. Indeed, the surface showed an LSPR absorbance peak at about 606 ± 0.6 (0.1%) nm with 0.446 ± 0.008 (1.8%) a.u. in intensity (Fig. 4A). This absorbance peak was not detected on the 2D-PC surface alone. Instead, a dip was observed at about 420 nm in the LSPR spectra (Fig. 3A). On the other hand, the Au-coated 2D-PC did not exhibit a reflectance signal around 400 nm (Fig. 4A). Therefore, the absorbance peak was produced from the LSPR of the uniform Au nanostructures on the surface.

DNA hybridization studies were also performed on this novel surface as a proof-of-principal. As ApoE probe ssDNA was immobilized on the Au-coated 2D-PC surface, both the peak wavelength and intensity increased to 628.3 ± 2.1 (0.3%) nm and 0.595 ± 0.042 (7.1%) a.u. respectively (Fig. 4B). The effective thickness of the adsorbate layer and electromagnetic decay length also affected the spectral shift of the system (Anker et al., 2008). This data implied a larger wavelength shift resulting from binding of more or larger biomolecules on the Au nanostructures. Similar effects of increased intensity and red-shift of LSPR peaks by biomolecular binding on the surface of Au nanoparticles were observed in previous biosensor applications (Cheng et al., 2015; Choi et al., 2014; Hsu et al., 2011; Lin et al., 2011).

When ApoE FC was incubated on the surface, a large increase in peak wavelength to 635.4 ± 1.4 (0.2%) nm and 0.941 ± 0.051 (5.4%) a.u was observed due to the formation of full hybrids. Other oligonucleotides such as MM and NC gave low LSPR responses of 632.8 ± 1.7 (0.3%) nm and 0.764 ± 0.024 (3.1%) a.u and 631.1 ± 1.8 (0.3%) nm and 0.644 ± 0.072 (11.2%) a.u, respectively.

This new sensor surface proved to have a higher specificity. This was attributed to the creation of strong LSPR characteristics on a uniformly ordered 2D-PC surface. A linear trend in the average LSPR peak wavelength was also obtained (Fig. 3B). NC incubation resulted in a LSPR signal, which highly overlapped with the probe, due to negligible binding, as expected. The slight red-shift in wavelength was attributed to the possible disruption of DNA film with the detergent-based washing steps.

4. Conclusions

In conclusion, we have demonstrated a simple and cost-effective technique for the detection of DNA hybridization using the NIL-based 2D-PC surfaces in ambient conditions. The film was fabricated uniformly using printable photonics technology. Direct detection of ApoE gene was performed on this film after dual-functionalization by observing Fresnel reflectance decrease. The uniformity of the surface was utilized to produce LSPR responses by coating a layer of Au on the 2D-PC surface. The specificity of ApoE gene detection was significantly improved using LSPR characteristics of the Au-coated 2D-PC surface. Based on this study, detection of real DNA samples isolated from the blood samples of AD patients will be performed employing this technique. Blood samples of AD patients will be collected from patients at various stages of disease progression. 2D-PC surfaces are highly promising for the development of miniaturized and cost-effective DNA sequence detection assays.

Acknowledgments

The authors gratefully acknowledge the financial support from Canada Foundation for Innovation (Project no: 35272), Ontario Ministry of Research and Innovation (Project no: 35272), Canada Research Chair (Tier 2) *"Bioelectrochemistry of proteins',* (Project no: 950-231116) and NSERC Discovery Grant (Project no: RGPIN-2015-3655) to K. K. We also appreciated Mr. Ben Hau's support in photographic images.

References

Ahmed, M.U., Idegami, K., Chikae, M., Kerman, K., Chaumpluk, P., Yamamura, S., Tamiya, E., 2007. Analyst 132, 431–438.
Aki, S., Endo, T., Sueyoshi, K., Hisamoto, H., 2014. Anal. Chem. 84, 11986–11991.
Alexeev, V.L., Sharma, A.C., Goponenko, A.V., Das, S., Lednev, I.K., Wilcox, C.S., Finegold, D.N., Asher, S.A., 2003. Anal. Chem. 75, 2316–2323.
Anker, J.N., Hall, W.P., Lyandres, O., Shah, N.C., Zhao, J., Van Duyne, R.P., 2008. Nat. Mater. 7, 442–453.
Aygun, U., Avci, O., Seymour, E., Urey, H., Unlu, M.S., Ozkumur, A.Y., 2017. ACS Sens. 2, 1424–1429.
Bellis, G.D., Salani, G., Panigone, S., Betti, F., Invernizzi, L., Luzzana, M., 1997. Clin. Chem. 43, 1321–1324.
Cheng, X.R., Hau, B.Y., Endo, T., Kerman, K., 2014. Biosens. Bioelectron. 53, 513–518.
Cheng, X.R., Wallace, G.Q., Lagugné-Labarthet, F., Kerman, K., 2015. ACS Appl. Mater. Interfaces 25, 4081–4088.
Choi, J.H., Lee, J.H., Oh, B.K., Choi, J.W., 2014. J. Nanosci. Nanotechnol. 14, 5658–5661.
Corder, E.H., Saunders, A.M., Strittmatter, W.J., Schmechel, D.E., Gaskell, P.C., Small, G.W., Roses, A.D., Haines, J.L., Pericak-Vance, M.A., 1993. Science 261, 921–923.
Cramer, P.E., Cirrito, J.R., Wesson, D.W., Lee, C.Y., Karlo, J.C., Zinn, A.E., Casali, B.T., Restivo, J.L., Goebel, W.D., James, M.J., Brunden, K.R., Wilson, D.A., Landreth, G.E., 2012. Science 335, 1503–1506.
de Harven, E., Leung, R., Christensen, H., 1984. J. Cell. Biol. 99, 53–57.
Deming, Y., Xia, J., Cai, Y., Lord, J., Holmans, P., Bertelsen, S., Holtzman, D., Morris, J.C., Bales, K., Pickering, E.H., Kauwe, J., Goate, A., Cruchaga, C., 2015. Neurobiol. Aging. http://dx.doi.org/10.1016/j.neurobiolaging.2015.09.009.
Ember, S.W., Schulze, H., Ross, A.J., Luby, J., Khondoker, M., Giraud, G., Terry, J.G., Ciani, I., Tlili, C., Crain, J., Walton, A.J., Mount, A.R., Ghazal, P., Bachmann, T.T., Campbell, C.J., 2011. Anal. Bioanal. Chem. 401, 2549–2559.
Endo, T., Ikeda, R., Yanagida, Y., Hatsuzawa, T., 2008a. Anal. Chim. Acta 611, 205–211.
Endo, T., Kajita, H., Kawaquchi, Y., Kosaka, T., Himi, T., 2016. Biotechnol. J. 11, 831–837.
Endo, T., Kerman, K., Nagatani, N., Takamura, Y., Tamiya, E., 2005a. Anal. Chem. 77, 6976–6984.
Endo, T., Ozawa, S., Okuda, N., Yanagida, Y., Tanaka, S., Hatsuzawa, T., 2010. Sens. Actuators B 148, 269–276.
Endo, T., Yamamura, S., Nagatani, N., Morita, Y., Takamura, Y., Tamiya, E., 2005b. Sci. Technol. Adv. Mater. 6, 491–500.
Endo, T., Yanagida, Y., Hatsuzawa, T., 2008b. Measurement 41, 1045–1053.
Farrer, L.A., Cupples, L.A., Haines, J.L., Hyman, B., Kukull, W.A., Mayeux, R., Myers, R.H., Pericak-Vance, M.A., Risch, N., van Duijn, C.M., 1997. J. Am. Med. Assoc. 278, 1349–1356.
Guo, L.J., 2007. Adv. Mater. 19, 495–513.
Guo, K., Li, X., Kraatz, H.-B., 2011. Biosens. Bioelectron. 27, 187–191.
Hsu, C.-Y., Huang, J.-W., Lin, K.-J., 2011. Chem. Comm. 47, 872–874.
Huang, C.J., Lin, Z.E., Yang, Y.S., Chan, H.W., Chen, W.Y., 2018. Biosens. Bioelectron. 99, 170–175.
Huang, C.S., Chaudhery, V., Pokhriyal, A., George, S., Polans, J., Lu, M., Tan, R., Zangar, R.C., Cunningham, B.T., 2012. Anal. Chem. 84, 1126–1133.
Hutter, E., Fendler, J.H., 2004. Adv. Mater. 16, 1685–1706.
Inan, H., Poyraz, M., Inci, F., Lifson, M.A., Baday, M., Cunningham, B.T., Demirci, U., 2017. Chem. Soc. Rev. 46, 366–388.
John, S., 1987. Phys. Rev. Lett. 58, 2486–2489.
Jon, S., Seong, J., Khademhosseini, A., Tran, T.-N.T., Laibinis, P.E., Langer, R., 2003. Langmuir 19, 9989–9993.
Jung, B., Frey, W., 2015. J. Nanosci. Nanotechnol. 15, 688–692.
Kaatz, M., Schulze, H., Ciani, I., Lisdat, F., Mount, A.R., Bachmann, T.T., 2012. Analyst 137, 59–63.
Kang, C., Phare, C.T., Vlasov, Y.A., Assefa, S., Weiss, S.M., 2010. Opt. Express 18, 27930–27937.
Kim, D.K., Kerman, K., Hiep, H.M., Saito, M., Yamamura, S., Takamura, Y., Kwon, Y.S., Tamiya, E., 2008. Anal. Biochem. 379, 1–7.
Landreth, G.E., Cramer, P.E., Lakner, M.M., Cirrito, J.R., Wesson, D.W., Brunden, K.R., Wilson, D.A., 2013. Science 340, 924.
Lee, S.M., Choi, K.C., 2010. Opt. Express 18, 12144–12152.
Lin, Y., Zou, Y., Lindquist, R.G., 2011. Biomed. Opt. Express 2, 478–484.
Liu, B., Ni, H., Zhang, D., Wang, D., Fu, D., Chen, H., Gu, Z., Zhao, X., 2017. ACS Sens. 2, 1035–1043.
Ma, Y., Di, J., Yan, X., Zhao, M., Lu, Z., Tu, Y., 2009. Biosens. Bioelectron. 24, 1480–1483.
McMahon, J.M., Emory, S.R., 2006. Langmuir 23, 1414–1418.
Marrazza, G., Chiti, G., Mascini, M., Anichini, M., 2000. Clin. Chem. 46, 31–37.
Marrazza, G., Tombelli, S., Mascini, M., Manzoni, A., 2001. Clin. Chim. Acta 307, 241–248.
Morris, J.C., Roe, C.M., Xiong, C., Fagan, A.M., Goate, A.M., Holtzman, D.M., Mintun, M.A., 2010. Ann. Neurol. 67, 122–131.
Ozkumur, E., Ahn, S., Yalcin, A., Lopez, C.A., Cevik, E., Irani, R.J., DeLisi, C., Chiari, M., Unlu, M.S., 2010. Biosens. Bioelectron. 25, 1789–1795.
Park, S., Lee, K.-B., Choi, I.S., Langer, R., Jon, S., 2007. Langmuir 23, 10902–10905.
Park, Y.-K., Park, S., 2008. Chem. Mater. 20, 2388–2393.
Sagle, L.B., Ruvuna, L.K., Ruemmele, J.A., Van Duyne, R.P., 2011. Nanomedicine 6, 1447–1462.
Sepúlveda, B., Angelomé, P.C., Lechuga, L.M., Liz-Marzán, L.M., 2009. Nano Today 4, 244–251.
Sharma, A.C., Jana, T., Kesavamoorthy, R., Shi, L., Virji, M.A., Finegold, D.N., Asher, S.A., 2004. J. Am. Chem. Soc. 126, 2971–2977.
Siest, G., Pillot, T., Régis-Bailly, A., Leininger-Muller, B., Steinmetz, J., Galteau, M.M., Visvikis, S., 1995. Clin. Chem. 41, 1068–1086.
Spuhler, P.S., Knezevic, J., Yalcin, A., Bao, Q., Pringsheim, E., Droge, P., Rant, U., Unlu, M.S., 2010. Proc. Natl. Acad. Sci. USA 107, 1397–1401.
Tel-Vered, R., Yehezkeli, O., Willner, I., 2012. Adv. Exp. Med. Biol. 733, 1–16.
Tombellis, S., Mascini, M., Braccini, L., Anichini, M., Turner, A.P., 2000. Biosens. Bioelectron. 15, 363–370.
Venter, J.C., et al., 2001. Science 291, 1304–1351.
Vlasov, Y.A., O'Boyle, M., Hamann, H.F., McNab, S.J., 2005. Nature 438, 65–69.
Wang, J., 2005. Small 1, 1036–1043.
Xu, X., Asher, S.A., 2004. J. Am. Chem. Soc. 126, 7940–7945.
Yablonovitch, E., 1993. J. Phys. Condens. Matter 5, 2443–2460.
Yurt, A., Daaboul, G.G., Connor, J.H., Goldberg, B.B., Unlu, M.S., 2012. Nanoscale 4, 715–726.